Full Configuration Low Boom Model and Grids for 2014 Sonic Boom Prediction Workshop

John M. Morgenstern,[*] Michael Buonanno[†] and Frank Marconi, PhD[‡]
Lockheed Martin Aeronautics Company, Palmdale, CA 93599

A conceptual supersonic transport design, identified as 1021-01, was developed for the NASA N+2 Supersonic Validations program. It was designed to produce very low sonic boom. A wind tunnel model was fabricated and tested to validate the predicted low sonic boom. An efficient "spatial averaging" measurement technique was used to handle distortions endemic to low sonic boom wind tunnel measurement, resulting in measurements precise enough to match predicted ground loudness within 1 PLdB. It was decided this model and data would make a good case for the 2014 Sonic Boom Prediction Workshop. Model development details and flow prediction challenges encountered during development are illustrated. Test oil flow visualization is shown to guide analyses, especially with regard to viscous boundary layer modeling. Viscosity was not important at full-scale but was found to be important at wind tunnel model scale (1/125). Geometry and grid files are expected to be available on the workshop website by 31 January 2013.

1. Background

In the late 1960's and 1970's the theory for shaping a vehicle for "Sonic Boom Minimization" (reference [ref.] 1) was invented by George, Seebass and Darden (ref. 2), to hopefully enable a supersonic transport (SST) to fly over land with acceptably quiet sonic boom. The theory and supporting methodology has been developed and refined since then up to the present, where we now believe we have the capability to design very low sonic boom vehicles.

The NASA N+2 Supersonic Validations Program sponsored wind tunnel testing to validate very low sonic boom designs. Early testing in the program revealed additional, wind tunnel flow field induced, measurement distortion challenges particular to such low, shaped sonic boom signatures (ref. 3). An efficient means was found to virtually eliminate these distortions by moving the model across the tunnel's spatially distributed distortions, while repeatedly measuring 20+ times, to average out the distortion effects (ref. 4). The resulting measurements (shown in section 3.4, figures 14-15, of this paper) were found to match within 1 PLdB (ref. 5). Based on its success, this model and data were selected as a case for the AIAA 2014 Sonic Boom Prediction Workshop.

This paper summarizes the design of this Lockheed Martin (LM) 1021-01 configuration to introduce its characteristics relevant to CFD analysis of the vehicle and its sonic boom. Model development analyses are shown to illustrate variations due to laminar versus turbulent viscous assumptions. Extensive oil surface flow photos are available and many are shown for comparison with CFD analyses and understanding of flow features.

2. Low Boom Model Design Development

2.1 Low Boom Design Process

The N+2 aft shock demo design effort was performed using a Rapid Conceptual Design (RCD) model that facilitates the prediction of sonic boom signatures using CFD. This model uses CATIA V5 for lofting and surface mesh generation, AFLR3 for volume grid generation, and can be used with multiple CFD solvers such as CFD++.

At the start of the N+2 design effort a combination of CFD++ and Optigrid (***Figure 1***) were respectively used for generation of the flow solution and adaptation of the volume grid to improve resolution of the sonic boom features. During the course of this design development, the model was significantly enhanced to incorporate superior flow solution and adaptation procedures, described further in section 2.2.

[*] N+2 Technical Manager, Advanced Development Programs, 1011 Lockheed Way B611 MC1142, AIAA Associate Fellow
[†] N+2 Program Manager, Advanced Development Programs, 1011 Lockheed Way B611 MC1142
[‡] N+2 Aero and CFD Senior Staff, Advanced Dev. Programs, 1011 Lockheed Way B611 MC1142, AIAA Associate Fellow

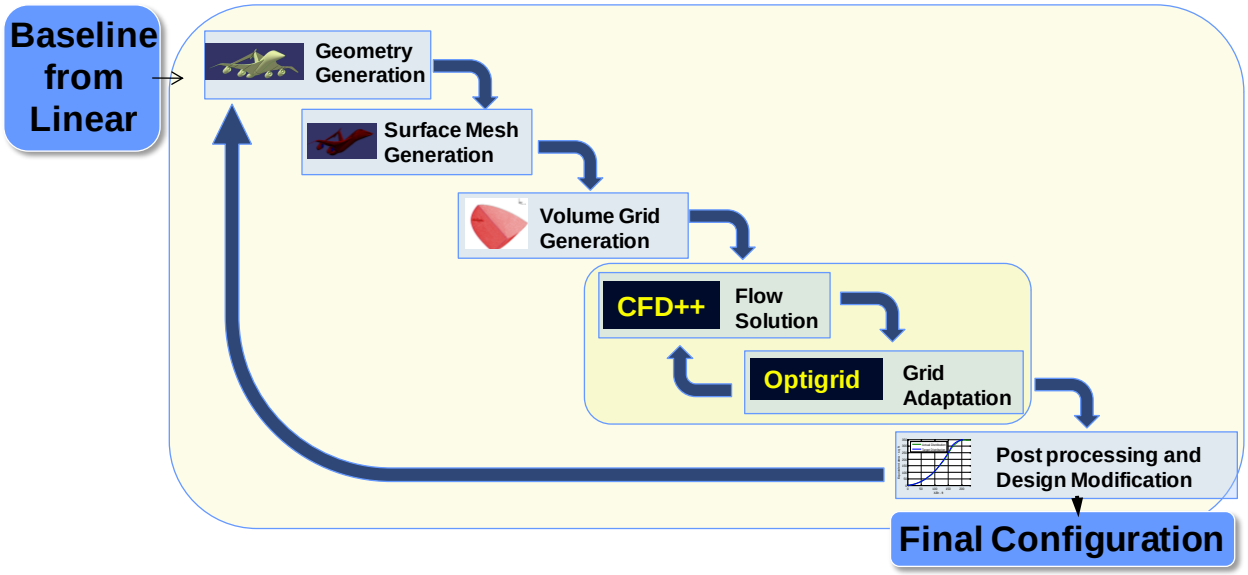

Figure 1. N+2 Design Tools Enabled Rapid Iteration of Low Boom Concepts.

The low boom design process begins with the creation of a parametric CATIA V5 loft that represents the essential features of the configuration being investigated (***Figure 2,*** *step 1*). The power copies CATIA command is used to rapidly generate different aircraft components with automatic joining and trimming, resulting in a watertight loft suitable for meshing (*step 2*). A surface mesh is then created from the loft in the CATIA V5 FMS workbench (*step 3*). Mesh parameters including size and structure are tailored to produce a quality surface triangulation with a reasonable number of elements suitable for rapid turn-around design work. For this program, surface triangulations were typically about 100,000 elements.

A major benefit of using the FMS license within CATIA for surface meshing, as opposed to traditional CFD meshing packages, is that the mesh is fully associative with the surface geometry, meaning new meshes can be generated "hands off". The surface mesh is then used to grow a volume mesh using AFLR3 (*step 4*). AFLR3 is a relatively robust tetrahedron grid generator that produces the UGRID files required by the different flow solvers used on the N+2 program.

2.2 Far-Field Correction and Stretched Prism Grid Improvements

LM's CFD-based sonic boom prediction needs are somewhat less stringent; we use a multi-pole far-field correction method (ref. 6) that allows us to extract a cylinder of CFD data at as little as 5 semi-spans [H/(b/2)] and correct it to a far-field propagation input. It provides the same results when used with accurate solution extractions from 5, 10 and 15 H/(b/2). Thereby, it can identify when a CFD solution is starting to lose resolution at farther distances, and indicates when a CFD solution is far enough away from the vehicle to be used for propagation without a far-field correction—when the far-field correction method no longer makes a difference to the propagation signature. We typically used solutions from 2.5 to 10 H/(b/2) for design work.

Both the NASA FUN3D and commercial CFD++ flow solvers were used to perform design work on the N+2 program. At the start of the program, CFD++ was used with the commercial feature-based grid adaptation program Optigrid to generate flow solutions for design studies. However, it was found to be difficult to tweak control parameters in Optigrid to achieve good results with distance from the body. The ability of FUN3D to perform adjoint-based adaptation led to its adoption for further work, and yielded a needed ten-fold

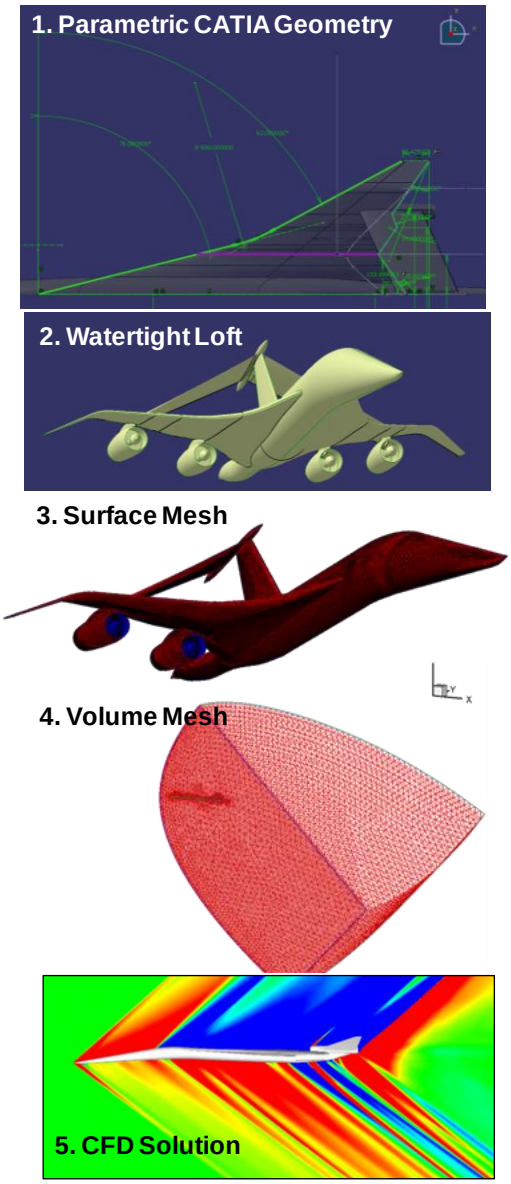

Figure 2. Associativity Between Parametric CAD and CFD Models Enables Rapid Generation and Evaluation of Low Boom Design Concepts.

improvement in sonic boom precision compared to the CFD++/Optigrid approach. Toward the end of the Phase I design work on N+2, a method inspired by work adopted by NASA was implemented in CFD++ that combines an unstructured grid around the vehicle with a structured grid of Mach-aligned stretched prisms, ***Figure 3***, ref. 7**.** This new method yielded results superior to those of the adjoint-adapted FUN3D approach, especially at greater distances, and at lower computational cost. This grid was developed for rapid design analysis turn-around, but the accuracy improvement that came from this grid topology turned out to be sufficient for wind tunnel matching without needing adaption or other refinement. Despite this sufficiency, running a refinement or adaption method (particularly on the inner, unstructured grid and complex vehicle aft end) may cause changes that further improve matching—improvement is possible.

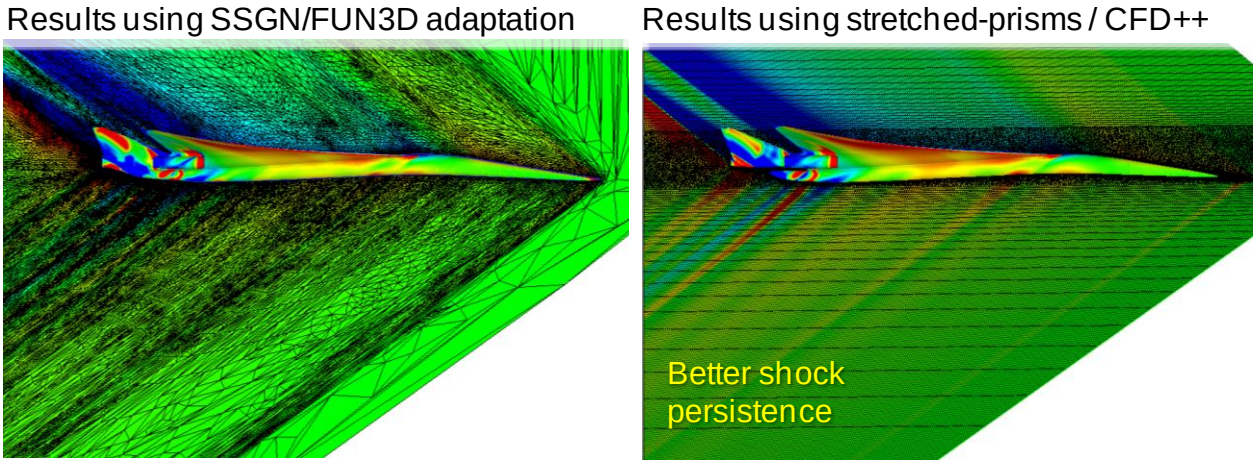

Figure 3. Both Adjoint-Based Adaptation and A-Priori Adaptation using Stretched Prisms were Applied during the N+2 Low Boom Design Process.

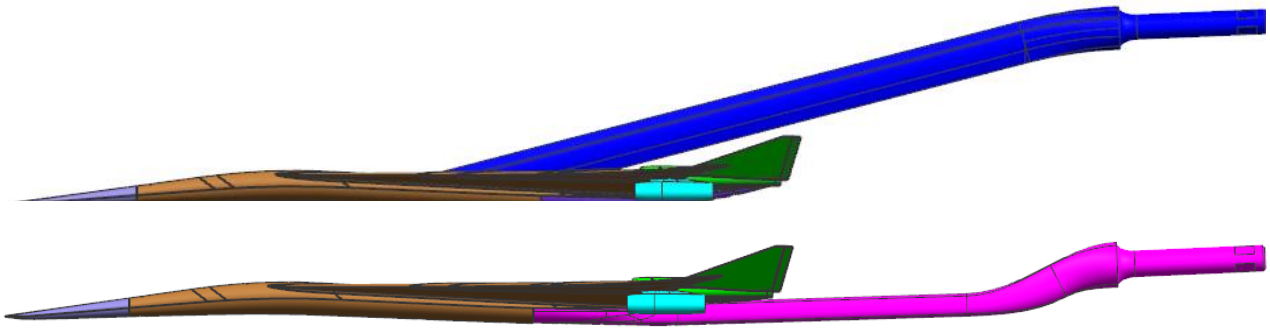

Figure 4. Both a Sting and Blade Model Support were Designed and Fabricated for the Low Boom Test to Reduce Risk due to Viscous Effects at Model Scale.

2.3 Model Design

Many analyses were performed to insure that the model would behave as intended. The model was built with both a blade support and sting support as shown in ***Figure 4***. The primary objective in this test was to get good aft shock measurements and the blade support offered less interference. However, several model analyses indicated 2 places where the flow was at risk for not matching the full-scale configuration due to viscous effects. Mostly these differences were observed when the boundary layer was run laminar. At the initially intended Reynolds number (Re#) of 2.55Million/ft, previous tests indicated that there was likely to be much laminar flow on a configuration this size. First, the blade support's front shock caused a vortex separation on the wing upper surface. Second, the wake from the blade support was causing choking from subsonic flow at the inlet of the centerline nacelle (***Figure 5***) that also induced another wing flow separation (***Figure 6***).

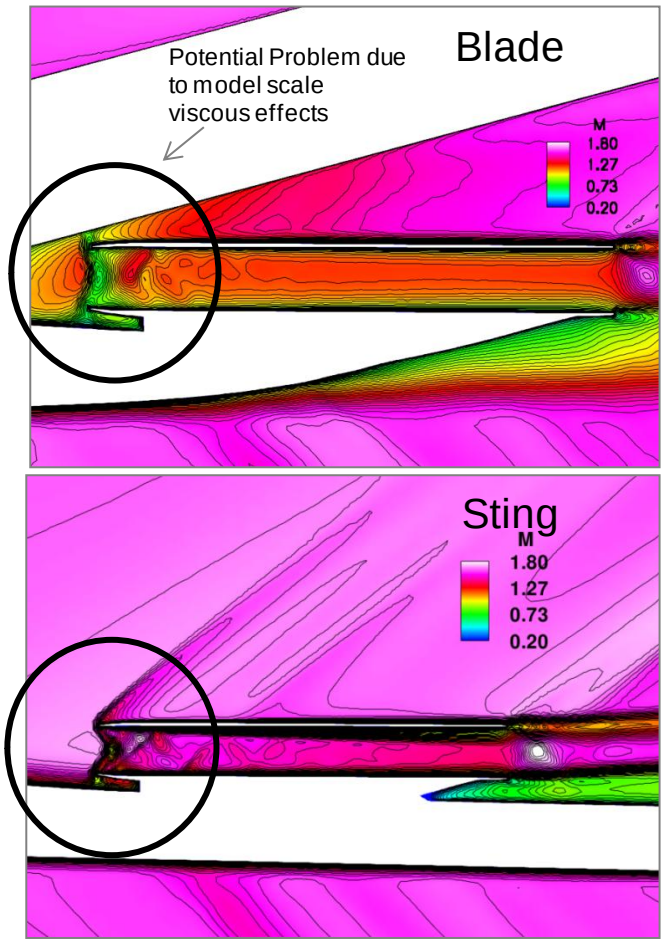

Figure 5. Viscous CFD Predictions Indicate the Potential for an Interaction Between the Blade Mount and the Centerline Nacelle.

Two changes might have worked against these laminar results coming to fruition. Trip discs were placed along the wing LE upper surface and along the blade at mid-chord, not necessarily sized to cause transition (0.006" height), but at least to energize the boundary layer to discourage flow separation (***Figure 7***). The test Re# was increased to 4.4M/ft because difficulty holding humidity constant at the lower Re# was causing more than 1/3 of the run time to be wasted. Test results seemed to match the Re# 2.55M/ft turbulent analyses much more closely than the laminar analyses, so turbulent analysis is recommended. Interestingly, laminar vortex separations were observed in surface oil flow during tunnel start-up when Re# was down near 1.4M/ft.

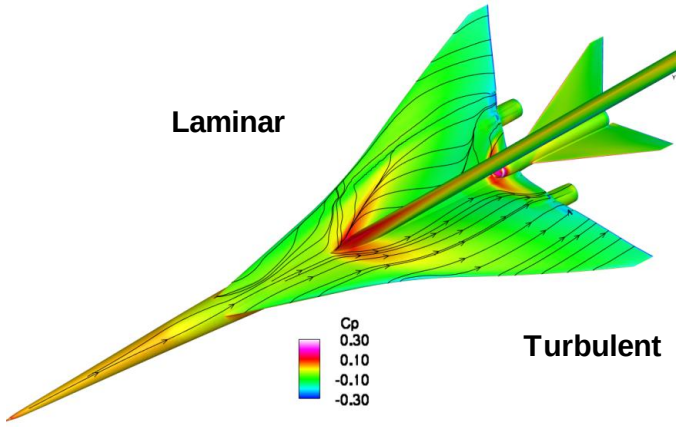

Figure 6. At Model Scale, Viscous CFD Results Indicate the Blade Support Induces Separation on the Wing Upper Surface if the Boundary Layer is Laminar, Suggesting the Use of Trip Discs to Discourage Separation.

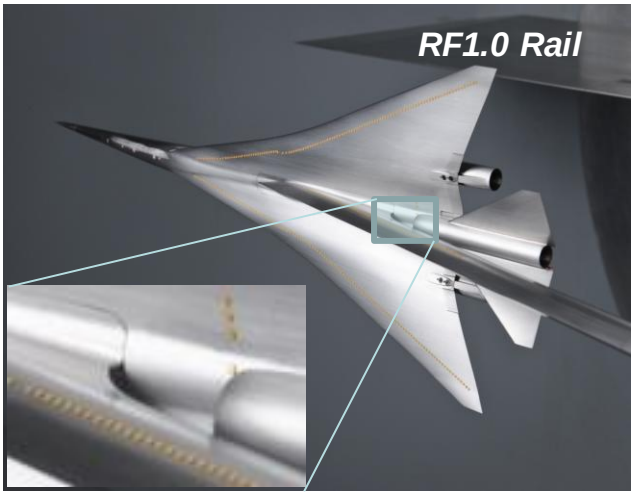

Figure 7. Model with Yellow Trip Discs, Inset Magnifies Blade Trip Discs and Unswept Blade Trailing Edge to Suppress Separation that Causes Nacelle Choking in Figure 5

2.4 Model Fabrication

The model was fabricated out of mostly 13-8 PH stainless steel by Tri Models, Inc., a specialist at wind tunnel model fabrication. Due to the small model size (although the largest sonic boom model to date, 22.4 inches [56.9 cm] in length) and sonic boom geometry sensitivity, meeting the desired tolerance was difficult. After fabrication, all parts are assembled and measured with an inspection machine. The match was remarkable with only 3 areas of discrepancies—predicted to be too small to change the propagated ground loudness significantly. In fact, the differences did not impact the propagated ground loudness and were not expected to even be measureable. However, the new "spatial averaging" measurement technique resulted in such precise measurements that signature differences were measured at discrepancy locations—too small to change loudness, but measureable. For thoroughness, we are looking into making an "as-built" geometry by modifying our "as-designed" geometry parametrically to closely approximate the discrepancies (with relatively minimal effort). Additional documentation or updates to this paper will be added to the Workshop website (ftp://lbpw-ftp.larc.nasa.gov/outgoing/) if the "as-built" geometry is the released geometry and for any other changes and updates. More details on the low boom configuration design development can be found in ref. 8 and ref. 9. (Refs. 3, 4 and 8 should also be available on the Workshop website.)

3. Low Boom Wind Tunnel Measurements

3.1 Test Description

Three Ames 9x7 wind tunnel entries have tested the sonic boom of the 1021-01 model (among many other models). The tests ran about 15 shifts each in October 2011, April 2012 and October 2012. The hardware set-up in the wind tunnel was the same for all and is illustrated in ***Figure 8***. The model blade is connected to a balance that connects to a linear actuator, which can translate the model up to 24 inches (61 cm). This model was built at its cruise angle-of-attack when the linear actuator is level, so height does not need adjustment during translation and minimal yaw adjustment with roll (due to flow angularity), speeding measurement productivity. A roll mechanism follows to allow measurement of off-track signature roll angles by the rail mounted on the wall. Testing is done sideways in the 9x7 because flow is more uniform in that plane. The RF1.0 "blade" rail has its pressure orifices on its "knife edge" 14 inches (36 cm) from the wall, avoiding reflections from the wall or the rail itself (1.0 reflection factor). The design of the RF1.0 rail (documented in ref. 10) was a key component of the measurement accuracy. Distances from 20 to 70 inches (50 to 177 cm) can be measured (with the limits occurring because this model gets ahead of the rail at closer distances, whereas the strut's motion limit and the far wall prevent further distances). Also, the rail must be remounted further aft in the tunnel to switch between measuring 20-42 inches (-107 cm) and measuring 42-70 inches distance. The tunnel strut translates in height (horizontally) so that the model can be held in place while angle-of-attack is changed; and for sonic boom, the strut allows easy variation of measurement distance from the rail.

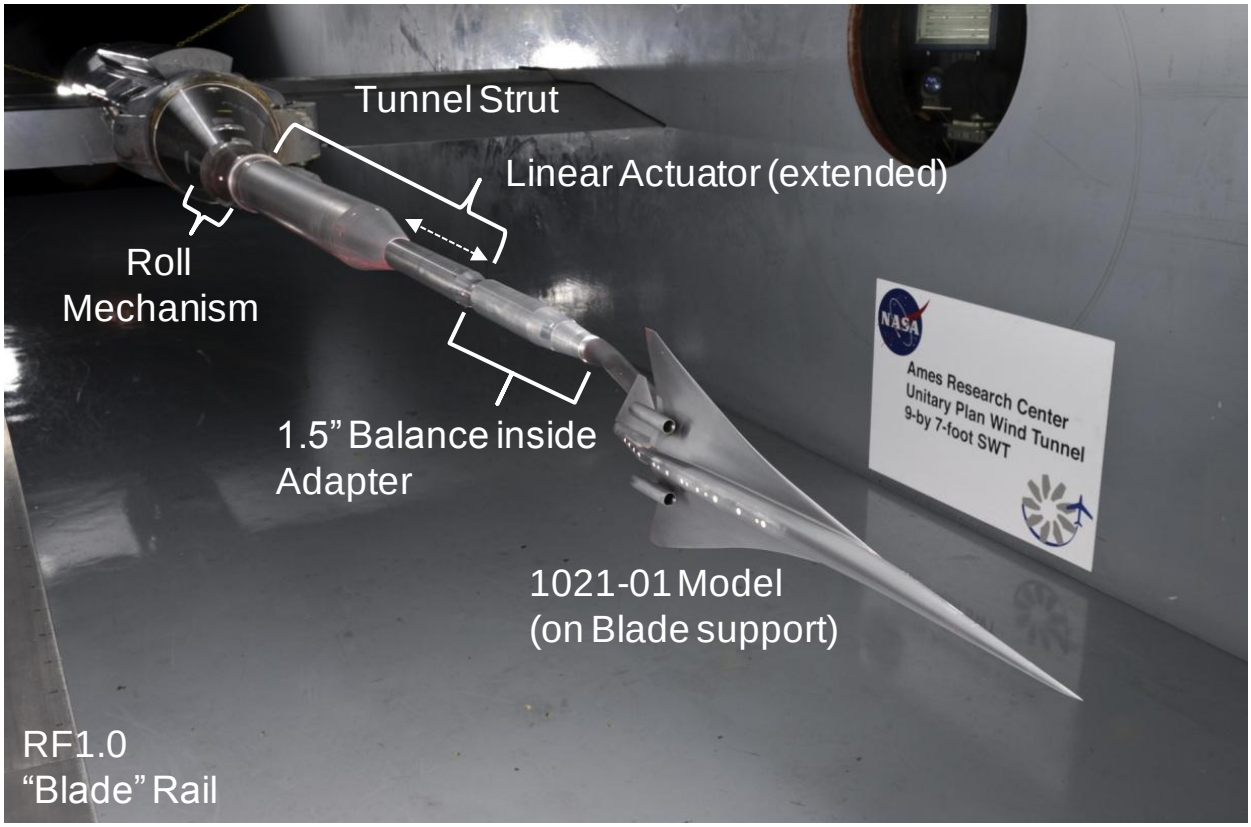

Figure 8. 1021-01 Model (on Blade), Balance and Actuation Hardware Components

3.2 Test Measurement Technique

The model is translated to get accurate sonic boom delta pressure measurements using a technique called spatial averaging, described in detail in ref. 4. To briefly summarize here, slight Mach variations of "shock diamonds," found in every supersonic wind tunnel test section, vary the local Mach angle enough to distort model delta pressure measurements ±20% at 20 inches to over ±50% at 70 inches. We found that averaging 20 or more equally spaced measurements over several periods of variation (several pairs of shock diamonds), whose length is 12 or more inches (25 cm) in this Ames 9x7 tunnel, is enough to virtually eliminate these distortions; but the averaging can round off detail. Measurement rounding already occurs due to model cantilevered vibration in the tunnel, typically about ±0.1 to ±0.3 inches. The blade mount is also preferred for this model because its greater pitch stiffness limited vibration toward a smaller ±0.15 inches. (Usually this vibration rounding is obscured in the first hundred yards/meters of propagation, due to signature aging's effect on shock slope.) Because of

measurement rounding, well resolved CFD analyses should have sharper shocks than wind tunnel measurements. Additional rounding from longer propagation through distortion begins impacting accuracy for distances greater than 42 inches (107 cm) in this tunnel. We are refining processing techniques to maintain accuracy out to 70 inches (177cm) and made calibration measurements like ref. 3. This distance is important because sonic boom propagation methodologies need starting signatures to be taken from beyond near-field distorted distances, which seems to ideally be 25 or more semi-spans away [25 H/(b/2), about equivalent to the legacy 5 H/L distance, where H is distance/height and L is vehicle length], but usually 15 semi-spans is enough to get similar ground signature loudness. For this configuration, H = 31.8 inch distance (81 cm) is H/(b/2) = 7.9 and H = 70 is H/(b/2) = 17.3, so the far distance measurement is desired for signature validation beyond the near-field. (For our predictions, we use our multipole far-field correction in all cases by mixing in predictions where measurements are missing.)

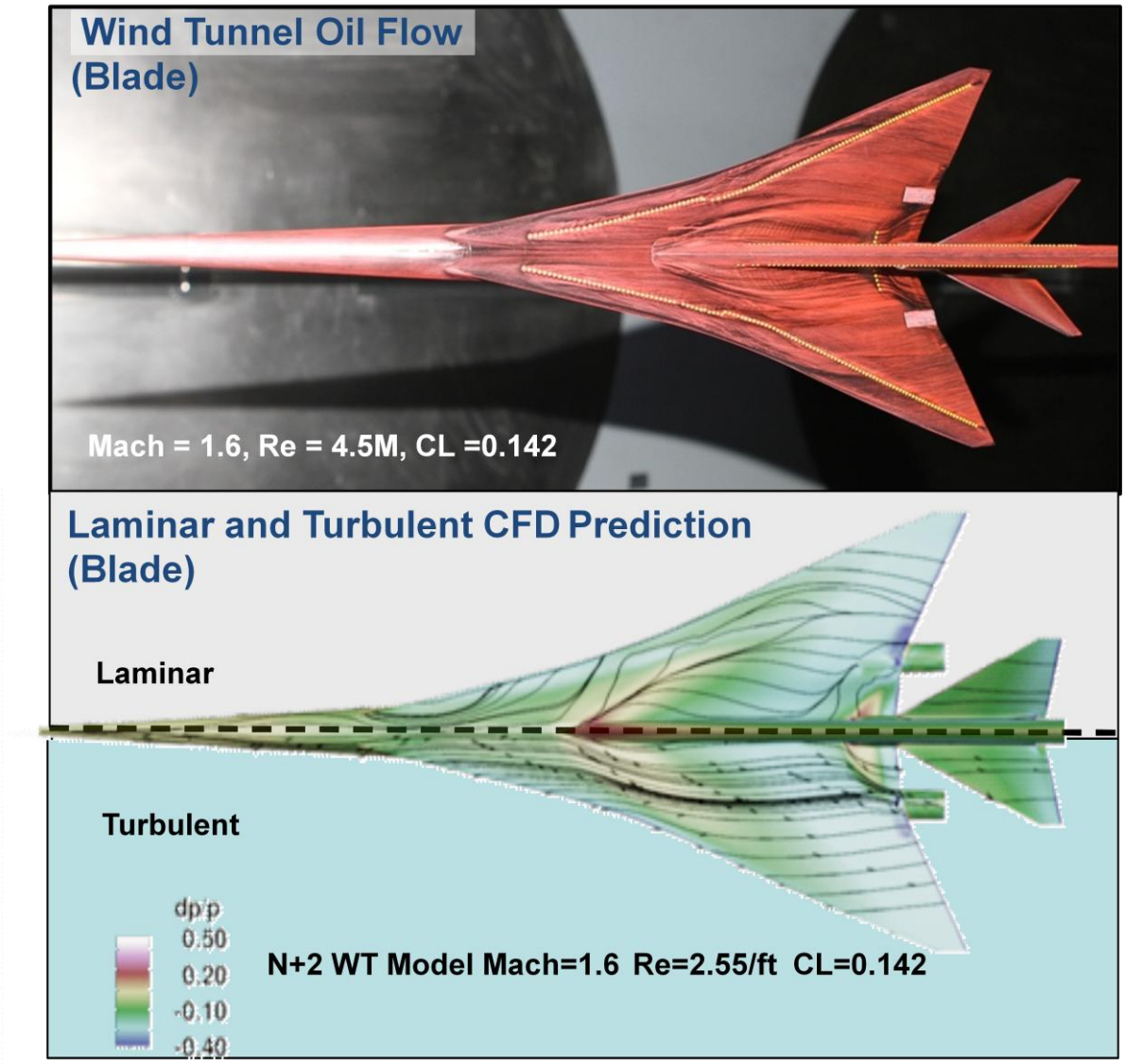

Figure 9. Oil Streaks Indicate Fully Attached Flow, Matching the Turbulent CFD

3.3 Oil Flow Visualization Comparisons

Oil surface flow visualization was used to assess whether the test flow-field was matching predictions. If the flow-field differed from predictions, oil surface flow would be likely to show the source of the difference—since we were mostly concerned about flow separation. Breaks in oil flow direction and non-streamwise flow can indicate locations of separation, which might suggest modeling changes (like boundary layer transition location) to better model the tunnel flow. As it turned out, running at either the original Re# of 2.55M/ft or 4.4M/ft, the flow stayed fully attached everywhere on the vehicle. Since the surface flow was matching the desired full-scale flow with the trip discs, we did not ever try to measure the model without trip discs. However, during initial supersonic flow at tunnel start-up when the Re# was only 1.4M/ft, separated flow (like the laminar boundary layer prediction in ***Figure 9***) was observed on the wing from the video monitor. (Watching this dynamically changing few minutes of separated flow finally explained some persistent streaks and shadow regions of more evacuated oil at

1/3 and at 2/3 of span ahead of the trip discs. Low Re# separation streaks also persisted in Figure 12.) Otherwise, the Figure 9 oil flow photo matches the turbulent prediction with its completely attached flow. Still images could also be taken from the video camera using UV lighting to fluoresce the red powder in the oil streaks, ***Figure 10***.

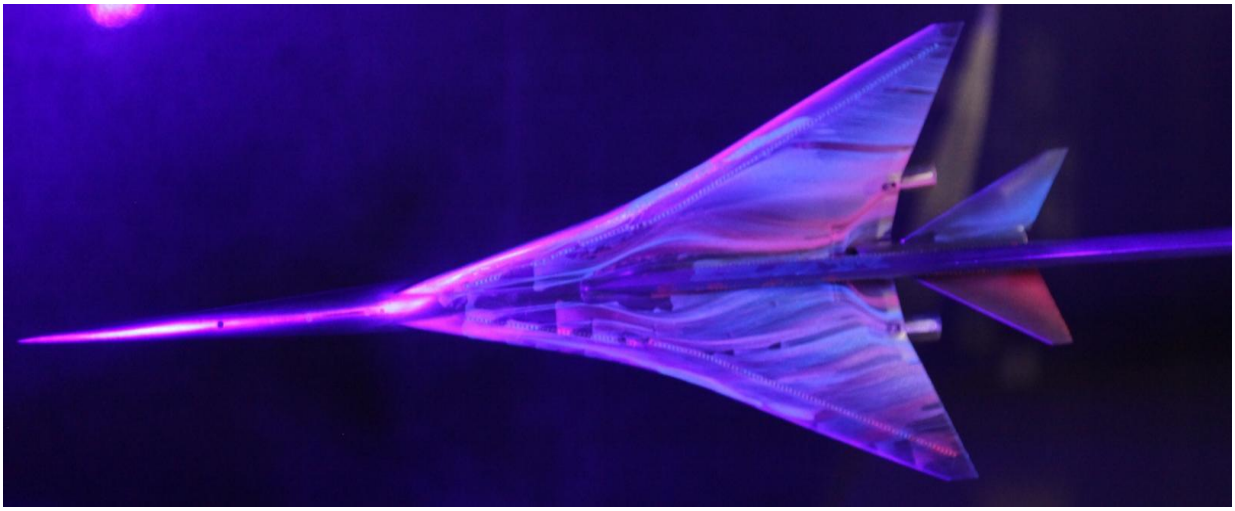

Figure 10. Video of Fluorescent Oil Flow Development were Taken Throughout Tunnel Start-Up Pattern changes

As stated previously, examination of the test oil flow patterns indicate attached flow everywhere at cruise conditions, similar to turbulent CFD analysis. To the contrary, past experience with transition detection by sublimation suggests that this model's boundary layer includes large laminar portions, and CFD using a laminar boundary layer predicts large separations. The lack of separation is probably due to three reasons. First, for the likely case of some mixed laminar and turbulent boundary layer regions, a recently transitioned boundary layer is even less likely to separate than a fully turbulent boundary layer. The trick is that the transition needs to occur before the adverse gradient that causes laminar separation. The second and third reasons act by encouraging transition: the trip discs on the model and tunnel flow turbulence (as opposed to the CFD's perfectly quiet ambient flow). Additionally, most of the test was run at a higher Re# than the CFD when it was found that test humidity was easier to hold at the higher pressure. (Better productivity more than offset the increased power cost.) The only significant region of separated oil flow was on the blade trailing edge, where it was expected to eventually occur but was intended to remain attached until above the center nacelle to avoid encouraging the choking shown in Figure 5. And the oil flow confirmed that the blade trailing edge flow remained attached until above the center nacelle, preventing reduced-Mach separated flow from un-starting the nacelle internal flow. In fact, the above separation appeared to be caused or at least increased by the center nacelle shock's strong, swept, adverse pressure gradient impingement, and may not have separated above the nacelle without the nacelle shock's impingement, ***Figure 11***.

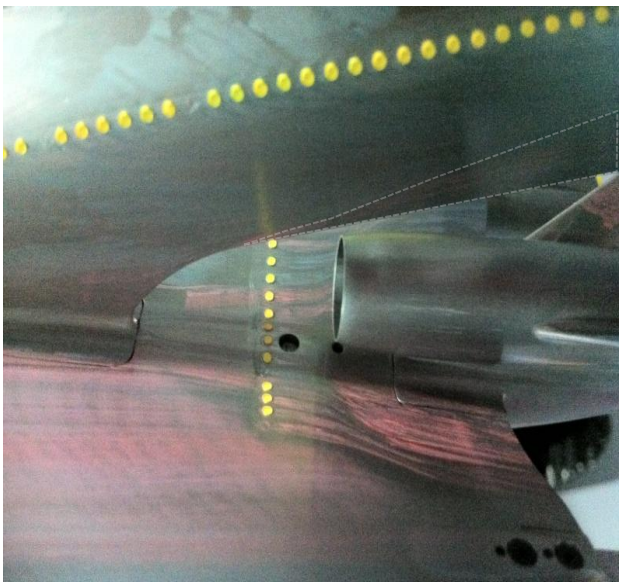

Figure 11. Blade Flow Attached Until Above Nacelle Inlet, Separation may Only Occur Because of Nacelle Shock Impingement

In the final October 2012 entry, a better UV light and photography equipment provided higher resolution pictures. The larger spacing of the trip discs seen on the vehicle upper surface in ***Figure 12*** was established near the end of the first entry. Sonic boom measurements for the workshop were all measured using this spacing. This spacing is more typical for highly swept wings and seeks to leave about a trip disc width of streamwise unimpeded flow between each disc. There seemed to be no measured effect on the data, while oil flow streaks became more visible and dramatic. The larger spacing was also applied to the blade, and shock waves from the blade discs were more strongly apparent on the inner wing as a rib-like pattern. The vehicle lower surface in ***Figure 13*** does not have streaks from trip discs, but the nacelle shocks' impingement on the wing and tails is apparent. Otherwise, flow is very streamwise and regular.

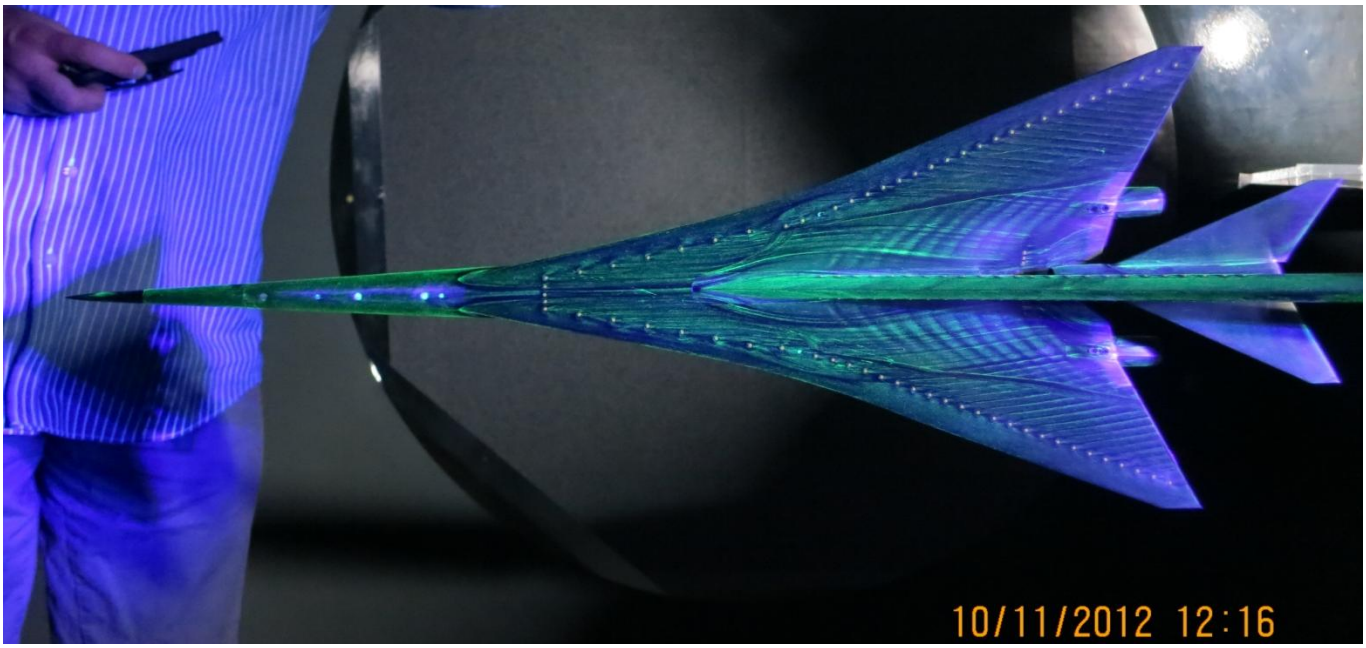

Figure 12. Improved Oil Flow Photography Resolution of Third Model Entry

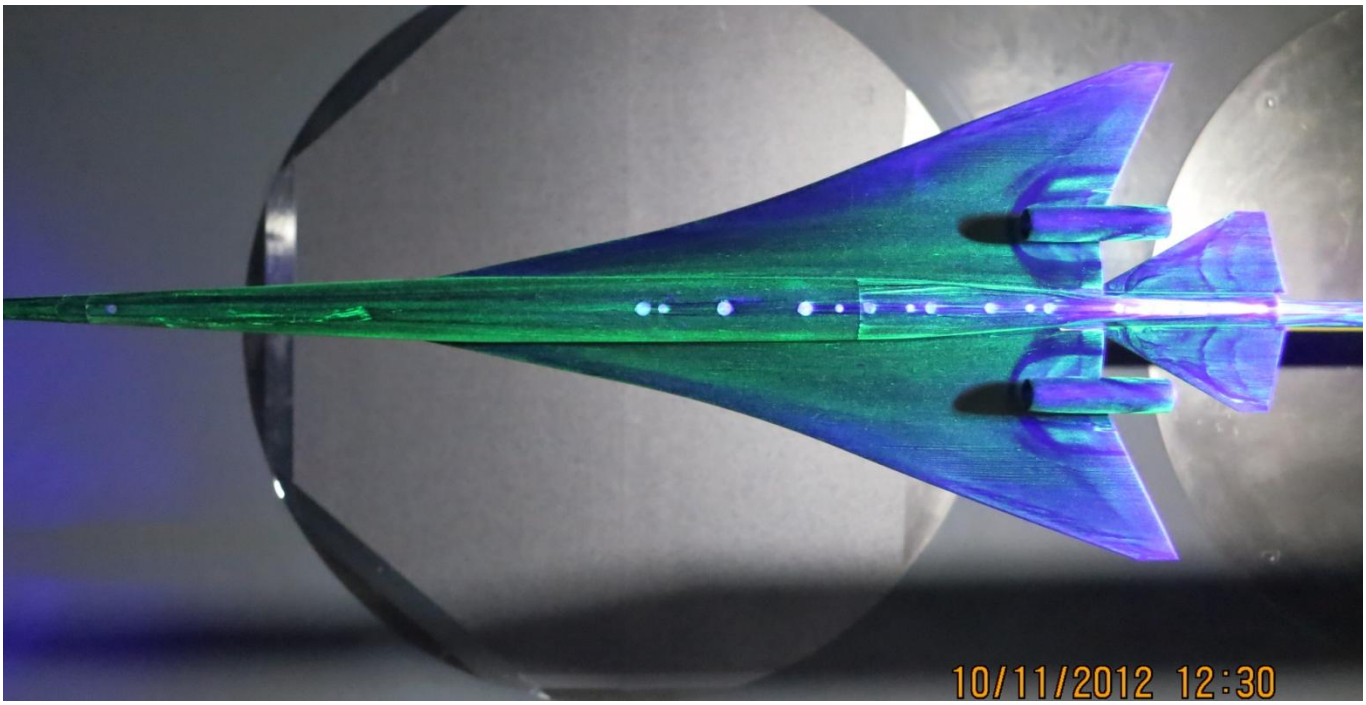

Figure 13. High Resolution Oil on Lower Surface Shows Nacelle Shock Effects on Wing and Tails

The predicted sonic boom difference between laminar and turbulent was small enough that either result would have been a good simulation of the full scale vehicle. The majority of the laminar flow field difference was shielded by the wing for sonic boom below the vehicle. Typically, having laminar flow on a sonic boom model (with attached flow still similar to full-scale) makes a better sonic boom match with the thin, full-scale boundary layer. At full scale, Euler predictions of sonic boom match viscous predictions because the boundary layer is so thin.

3.4 Sample Signature Measurement

The first test entry signature measurements yielded remarkable CFD / low boom measurement matching using the first application of the spatial averaging technique. ***Figure 14*** provides one measurement condition, at two CL's, as a one and only pre-workshop check case. The upper left corner plot shows the compilation of measurements that were averaged to make the final signature. This signature was already shown in refs. 3, 4, 8 and 9, so it is re-shown here for pre-workshop comparison. This signature measurement was taken at H = 31.8 inches. (One caveat, improvements in signature processing are being

worked, so a newer processing of this case could change to a slightly sharper signature.) To quantify the accuracy of this match in loudness, the prediction and measurement of ***Figure 14*** were propagated to the ground and run through a loudness analysis. As shown in ***Figure 15*** (a.k.a. Figures 48 and 49 of ref. 8), the results were less than 1 PLdB different.

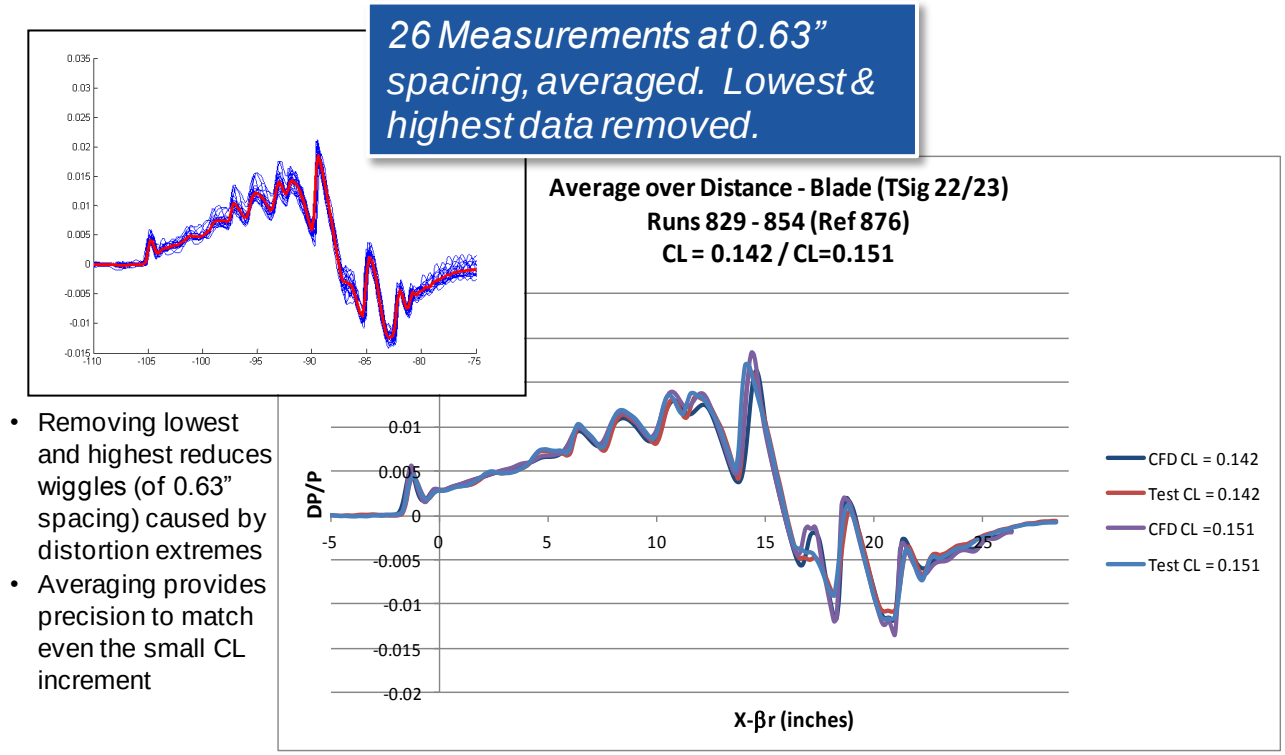

Figure 14. Pre-Test CFD Matches Measurement with Remarkable Precision

4. Full Configuration Prediction Case Description

4.1 Geometry and Sample Grid Files

The geometry will be in a step file format (.stp) created in CATIA V5. The recently added opportunity to use an "as-built" geometry version described earlier (section 2.4 Model Fabrication) does mean the geometry is not yet available. It is expected to be ready for download by the end of January. Details of the geometry will be posted on the website along with the geometry and the model assembly drawing sheet with the desired reference quantities, also shown in miniature in ***Figure 16***.

The initial sample grid will be of the mixed unstructured tetrahedral near and structured prism farther away described in section 2.2. Attempts will be made, but other grid formats will only be provided where outside support for their generation can be obtained. Since it is the goal of the workshop to document best practices for sonic boom prediction, generation of your own grids and analyses is particularly desired and appreciated.

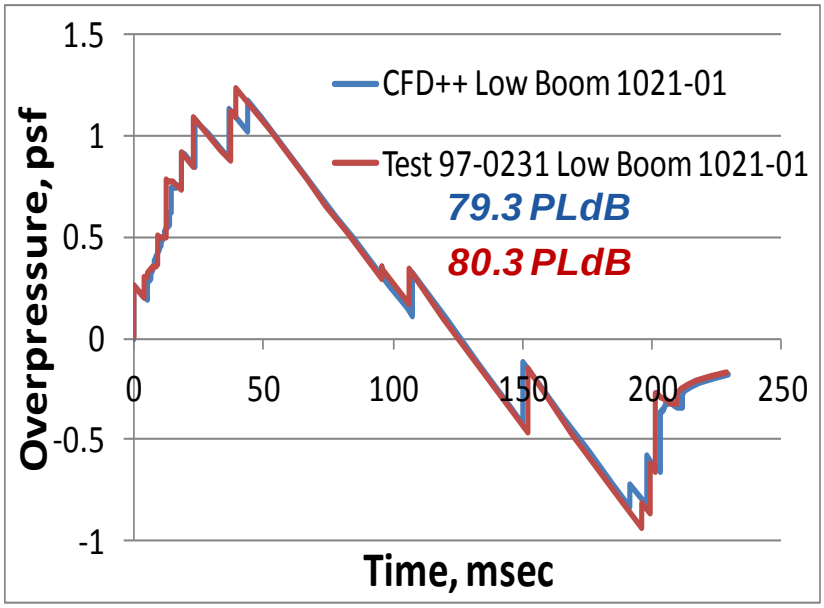

Figure 15. Propagation of Figure 14 Prediction and Measurement Match Within 1 PLdB

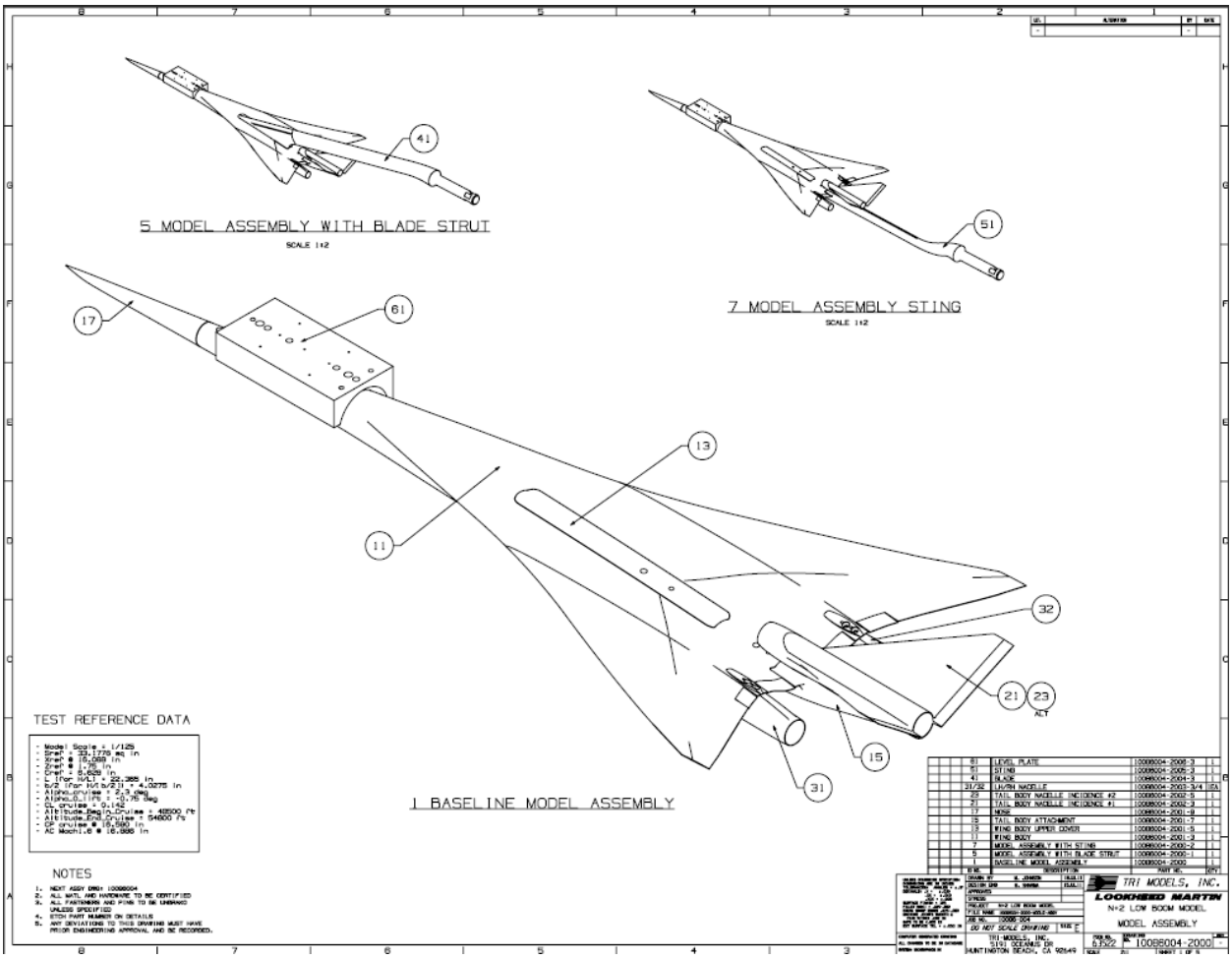

Figure 16. Assembly Drawings of the LM N+2 Low Boom Model and Support Hardware

4.2 Available Signature Measurement Conditions and Locations

All measurements that will be available for comparison were taken at Mach 1.6, Re# 4.4M/ft, Pstatic = 541 psf, Q = 970 psf. The model reference conditions to use are documented on its drawing sheet, and copied in the Figure 16 table for convenience. One nice characteristic of sonic boom prediction comparison is that only one CFD solution is needed to match the 19 measurements listed in the first six rows of the table below. The 31.8 height at 0 roll angle is the measurement already provided in section 3.4. These other 18 measurement comparisons will be made at the workshop plus 7 more conditions will be compared against a reference prediction to compare CFD prediction out to an H/(b/2) = 25. An alternate CL is provided since it is available and is an important parameter for low boom.

Distance (H), in	Alpha	CL	H/(b/2)	Roll Angles, degrees
69.6	2.30	0.142	17.3	0, 10, 20, 30, 40, 50 and 60
59.9	2.30	0.142	14.9	0
51.0	2.30	0.142	12.7	0
42.0	2.30	0.142	10.4	0 and 40
31.8	2.30	0.142	7.9	0, 10, 20, 30, 40, 50 and 60
19.7	2.30	0.142	4.9	0
Bonus				(prediction comparison only)
100.7	2.30	0.142	25.0	0, 10, 20, 30, 40, 50 and 60
Alternate CL				
31.8	1.93	0.125	7.9	0 and 40

TEST REFERENCE DATA

Model Scale = 1/125
Sref = 33.1776 sq in
Xref @ 16.088 in
Zref @ 1.75 in
Cref @ 6.628 in
L (for H/L) = 22.396 in
b/2 (for H/[b/2]) = 4.027 in
Alpha_cruise = 2.3 deg
Alpha_0_lift = -0.75 deg
CL cruise = 0.142
Altitude_Begin_Cruise = 48500 ft
Altitude_End_Cruise = 54800 ft
CP cruise @ 16.590 in
AC Mach 1.6 @ 16.886 in

Figure 17. Model Test Reference Quantities from the Model Drawing Sheet and Repeated Here for Convenience

When extracting DP/P information for comparison, the data should be extracted along the flight path, or in other words, at Alpha = 0, or at Alpha degrees less in pitch than the vehicles reference longitudinal axis. For this case, distance should be measured (H inches) from the vehicle's Xref, Y=0, Zref.

For example for the first table case,

Z = Zref – 69.6 = -67.85, Y = 0, X should be plotted with β*H subtracted (typical X – β*R axis, β=sqrt[M^2-1])

For the second table case

Z = Zref – 69.6 cos (10 deg) = -66.79, Y = 69.6 sin(10 deg) = 12.09.

Acknowledgements

The work described herein was done under a NASA contract from NRA ROA-2008 Topic A.4.4 "System-Level Experimental Validations for Supersonic Commercial Transport Aircraft." The authors would like to thank Clayton Meyers, Linda Bangert and Peter Coen for their input, feedback and support of this work, and the following other NASA personnel. Susan Cliff for her design and analysis of the RF1.0 rail, CFD boom analyses of many geometries, guidance with CFD sonic boom prediction, adjoint adaptation and test support helping to spot distortion patterns and identifying better "reference after measurement." Don Durston and Bruce Storms for the new Linear Actuator, test planning and test support helping to spot distortion patterns. Maureen Delgado for her test management skill and the skill of the whole Ames facility team. Eric Walker for his test support and skill with statistical analysis methodology to visualize distortion patterns and repeat and enhance the spatial averaging calculations in Matlab scripts used for some of the analysis herein. And from LM, Bob Langberg for his expert help with test planning, support and day-shift oversight. And from Tri Models, their team for the excellent fabrication quality of the RF1.0 rail, Linear Actuator and the highest precision model, 1021-01, to date.

References

1. George, A.R., and Seebass, R, "Sonic Boom Minimization Including Both Front and Rear Shocks," *AIAA Journal.* 9 (10), 2091-2093, October 1971.
2. Darden, C.M., "Sonic Boom Minimization With Nose Bluntness Relaxation," NASA TP 1348, 1979.
3. Morgenstern, J.; "Distortion Correction for Low Sonic Boom Measurement in Wind Tunnels," AIAA-2012-3216, 30th Applied Aerodynamics Conference, June 2012.
4. Morgenstern, J.; "How to Accurately Measure Low Sonic Boom in Supersonic Wind Tunnels," AIAA-2012-3215, 30th Applied Aerodynamics Conference, June 2012.
5. Stevens, S.S., "Perceived Levels of Noise by Mark VII Decibels (E)," *J. Acoust.Soc. Am*., Vol 51, No. 2, Pt. 2, Feb 1972, pp 575-601.
6. Page, J.A. and Plotkin, K.J. "An Efficient Method for Incorporating Computational Fluid Dynamics Into Sonic Boom Prediction," AIAA 91-3275, 9th Applied Aerodynamics Conference, September 23-25, 1991.
7. Ishikawa, H.; Tanaka, K.; Makino, Y. and Yamamoto, K.; "Sonic-Boom Prediction Using Euler CFD Codes with Structured / Unstructured Overset Method," 27th ICAS, 2010.
8. Morgenstern, J.; Buonanno M. and Norstrud, N.; "N+2 Low Boom Wind Tunnel Model Design and Validation," AIAA-2012-3217, 33rd Applied Aerodynamics Conference, June 2012.
9. Norstrud, N; Morgenstern, J.; Buonanno, M. and Sunny, C.; "N+2 Supersonic Validations Final Report – Phase I," NASA CR-xxxx-xxxxx (not yet published), 2012.
10. Cliff, S.; Elmiligui, A.; Aftosmis, M.; Thomas S.; Morgenstern J. and D. Durston, D.; "Design and Evaluation of a Pressure Rail for Sonic Boom Measurement in Wind Tunnels," ICCFD7-2006, Seventh International Conference on Computational Fluid Dynamics, Big Island, Hawaii, July 9-13, 2012.